Towards LC SQUID thermometry: measuring sub-Kelvin temperatures with high frequency noise

THESIS

submitted in partial fulfillment of the
requirements for the degree of

BACHELOR OF SCIENCE
in
PHYSICS

Author :	I.S. Kuijf
Student ID :	s2024802
Supervisor :	Prof.dr.ir. T.H. Oosterkamp
2^{nd} corrector :	Dr. W. Löffler

Leiden, The Netherlands, June 19, 2020

Towards LC SQUID thermometry: measuring sub-Kelvin temperatures with high frequency noise

I.S. Kuijf

Huygens-Kamerlingh Onnes Laboratory, Leiden University
P.O. Box 9500, 2300 RA Leiden, The Netherlands

June 19, 2020

Abstract

To find good upper bounds for the CSL model by measuring the force noise on a cantilever, the thermal noise should be minimized. To achieve millikelvin temperatures a nuclear demagnetization stage can be used, which should be thermally connected to the cantilever through a heat link. In this thesis we attempt to design a thermometer for sub-Kelvin temperatures to test this future heat link. The thermometer designed consists of an LC resonator with a high Q factor placed in series with the input coil of a dc SQUID. The inductor used is a 270 ± 5 μH niobium wire inductor and the capacitor is an 80 pF niobium plate capacitor. A metal foil is coupled to the resonator coil, which limits the Q factor and induces a Johnson noise in the coil according to the fluctuation dissipation theorem. This thermometer should work for temperatures down to 1 mK. However, we were not able to measure a resonance peak with the resonator attached to the SQUID input coil. To find the cause of this and determine if this thermometer design is viable, more research is needed.

Contents

Version of June 19, 2020– Created June 19, 2020 - 18:48

Chapter 1

Introduction

Over the past century there has been a growing interest in quantum mechanics. Being able to detect and manipulate quantum mechanical particles gives rise to a lot of new technologies, but how does quantum mechanics really work? An important part of quantum mechanics is the existence of the quantum mechanical wave function, which is a mathematical description of the quantum state of a particle. If a measurement is done on this particle, its wave function collapses into one of the states of the measurement basis. This collapse can be experimentally tested and has been observed numerous times. But what classifies as a measurement? What exactly causes this observed collapse?

Numerous interpretations and theories of quantum mechanics have been proposed. A group of theories that aim to explain the wave function collapse are the objective-collapse models, also known as spontaneous localization models. Those models state that the wave function collapse is a physical event, the localisation of a particle, which is continuously happening and may also occur on its own without a measurement needing to be done. One of those models is the continuous spontaneous localisation (CSL) model. This is a white-noise model, which means that a white-noise field is thought to be the cause of the spontaneous collapses [1].

CSL predicts a tiny violation of energy conservation, as a result of the wave function collapse generating a bit of heat. This is similar to the fact that a projection operator does not conserve energy. Vinante et al. came up with a way to measure this violation by using a millikelvin cooled mechanical resonator [2]. This mechanical resonator is implemented as an ultrasoft, magnetically tipped nanocantilever. According to the equipartition theorem the mechanical resonator's kinetic energy should be the same as its thermal energy. The temperature of the cantilever can thus be measured

Version of June 19, 2020– Created June 19, 2020 - 18:48

through the force noise on the cantilever. In thermal equilibrium, without the energy conservation violation, the measured temperature would then be the same as the temperature of the environment. This experiment can be used to test CSL and determine upper bounds for the single particle collapse rate λ at different values for the characteristic length r_C. Those λ and r_C are characteristic parameters of the CSL model.

To find good upper bounds for the CSL model and its small energy conservation violation, all other noise sources that can contribute to the force noise such as thermal radiation from higher temperatures and mechanical disturbance should be minimized. The mechanical disturbance can be reduced by suspending the cantilever from a mass spring system. To make the thermal radiation noise negligible, radiation coming from higher temperatures should be shielded or filtered. Very low temperatures down to $\sim$10 mK can already be achieved with a dilution refrigerator, but to be able to cool the cantilever down even further, a nuclear demagnetization stage (NDS) can be used. In nuclear demagnetization a magnetic field is applied to a refrigerant while keeping the temperature constant. This will make the nuclear spins align, decreasing the entropy. When the magnetic field is then adiabatically decreased, the temperature will decrease as well. The refrigerant can now be used to cool down the cantilever. While absorbing heat from the cantilever, the nuclear spins reorient themselves while the entropy and temperature increase to the initial values.

To be able to cool the cantilever down further with the NDS, a heat link between the NDS and cantilever should be designed and tested. The magnet of the NDS is placed higher up in the refrigerator, between the 50 mK plate and the 1 K plate (still plate). The refrigerant is inside the magnet but thermally connected to the 10 mK plate (mixing chamber plate) through a thermal conductance switch. The mechanical resonator is suspended from a mass spring system, which is attached under the mixing chamber plate. The dilution refrigerator and the NDS and cantilever placement are shown in figure 1.1. The heat link should thus be run through the mixing chamber plate, and along the mass spring system. It is critical that there are no heat leaks along this path, which is about half a meter long. To avoid introducing mechanical disturbances through the heat link, the link should also be attached to each layer of the mass spring system, where the contacts should not leak too much heat.

To be able to test the heat link we will need to do low temperature thermometry. In this thesis the main aim will be to design a SQUID thermometer that could be used to test this heat link. The thermometer should thus be able to accurately measure temperatures ranging from 1 mK to 1 K. Theory needed to understand the thermometer is given in chapter 2.

Version of June 19, 2020– Created June 19, 2020 - 18:48

Chapter 3 shows the making and testing of the LC resonator part of the thermometer. Chapter 4 shows the testing of the thermometer for sub-Kelvin temperatures, and chapter 5 further discusses the results and outlook.

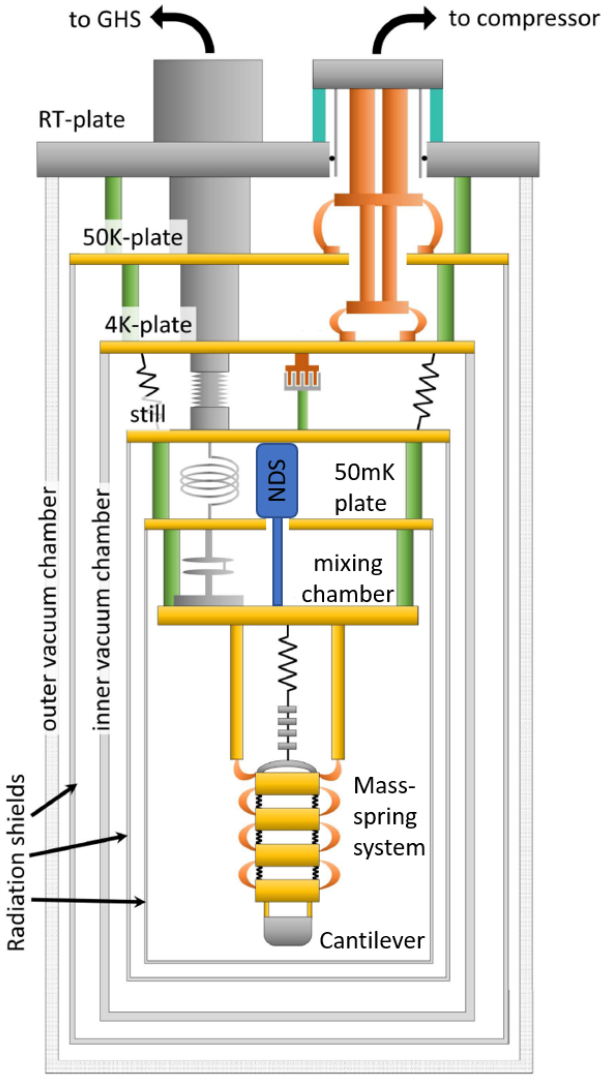

Figure 1.1: *Schematic of the dilution refrigerator. The different plates are indicated in the figure. The NDS and cantilever placement are also indicated. Adjusted from [3].*

Chapter 2

Theory

In this chapter we will show some theory useful for understanding the thermometer. Section 2.1 briefly discusses different types of thermometry and the general principle of SQUID thermometry, to explain why we chose to do thermometry this way. Section 2.2 gives some theory about the SQUID we will be using, and section 2.3 gives theory about the quality (Q) factor.

2.1 Thermometry

To be able to check the heat link we will need a thermometer that can measure sub-millikelvin temperatures. There are different types of thermometers we could use for this. Two examples that can measure these low temperatures are a CMN thermometer and SQUID thermometry. A CMN thermometer uses the temperature dependence of the susceptibility of powdered Cerium Magnesium Nitrate (CMN) [4]. A set of detector coils is used to produce a signal proportional to the susceptibility. This type of thermometer can be calibrated with several reference points. Good reference points for thermometry can be provided by a Superconductive Reference Device (SRD) sensor [4]. An SRD sensor uses transitions between the superconducting and the normal state of various materials to establish reference points.

Although CMN thermometry is an easy way to measure low temperatures, we will be using SQUID thermometry. Reasons for this are that a SQUID thermometer has a wider temperature range, is easier to develop ourselves and may be integrated with our SQUID sensors for cantilever motion in the future. The aim of the SQUID thermometer is to measure the

temperature of a piece of metal. Usually, the thermometer is operated in dc mode and the low frequency Johnson noise of the electrons in the metal are measured (figure 2.1(a)). The noise is measured up to a cut off frequency (typically lower than 1kHz) determined by the effective resistance of the metal and the inductance of the superconducting circuit including the coil that inductively couples to the metal and the SQUID input coil [5]. We will refer to this type of SQUID thermometer as an LR thermometer. Working at such low frequencies makes the LR thermometer susceptible to mechanical interference.

To avoid this interference, we aim to use a SQUID thermometer at higher frequencies. To achieve this, we add a capacitance in series with the inductor to get an LC resonator (figure 2.1(b)). The metal of which we want to measure the temperature is still coupled to the coil as before, but now it shows up as limiting the Quality (Q) factor of the LC resonator. The Q factor is the ratio of energy stored to the energy dissipated in the resonator in a single period. We will refer to this type of thermometer as an LC thermometer. With the LC thermometer the surface of the high frequency resonance peak can be measured to determine the temperature, instead of measuring the low frequency noise spectrum with an LR thermometer.

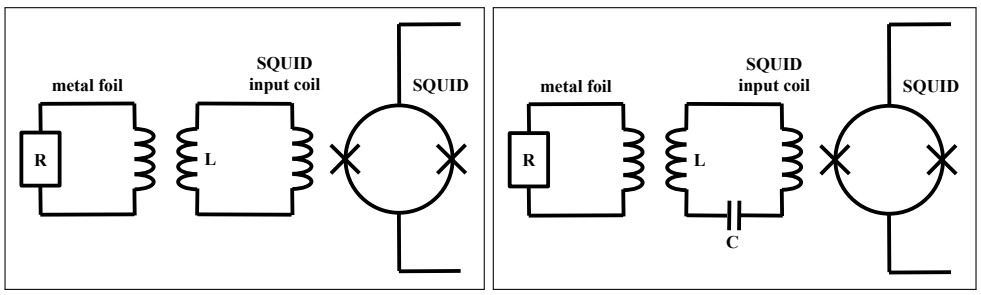

(a) *Schematic LR thermometer* ***(b)*** *Schematic LC thermometer*

Figure 2.1: *Schematics of the SQUID LR thermometer (a) and the SQUID LC thermometer (b). The metal foil is inductively coupled to the coil and is represented as an inductance in series with a resistance.*

2.2 SQUIDs

To measure the small current produced by the Johnson noise in the metal foil, we use a SQUID. A SQUID (SuperConducting QUantum Interference Device) is a very sensitive magnetometer, consisting of a superconducting loop with two parallel Josephson junctions. There are two main types of

Version of June 19, 2020– Created June 19, 2020 - 18:48

SQUIDS. One is the direct current (dc) SQUID, which is the type we will be using, and the other is the radio frequency (rf) SQUID. The rf SQUID consists of a single junction in a superconducting loop, making it cheaper than the dc SQUID, but also less sensitive. In order to understand the physics behind the SQUID thermometry, we will now briefly discuss the theory behind the dc SQUID. This section is based on The SQUID Handbook by Clarke and Braginski [6]

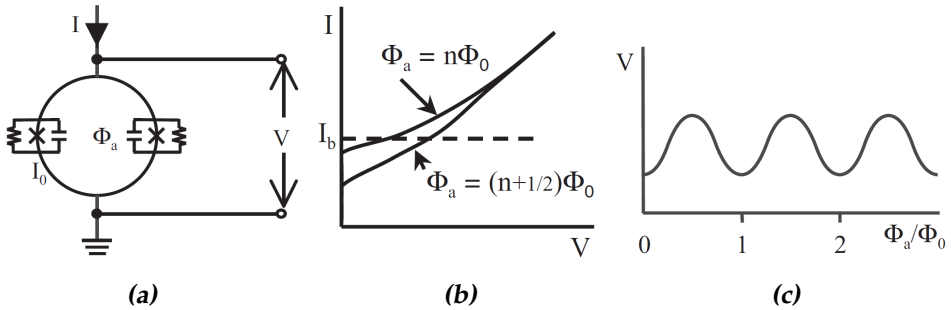

Figure 2.2: *The dc SQUID. (a) shows a schematic of the superconducting ring with the two Josephson junctions enclosing a magnetic flux Φ_a. The critical current of the Josephson junctions is I_0. A bias current I is applied to the ring and voltage difference V is measured. (b) shows a the I-V characteristics of the SQUID at integer and half-integer flux quanta and a bias current I_b for a good working point. (c) shows a typical V-Φ_a characteristic of the dc SQUID. Images adapted from [6].*

The dc SQUID consists of a superconducting ring with two Josephson junctions connected in parallel, biased with a current I. A schematic of the circuit is shown in figure 2.2(a). If a magnetic flux Φ_a is enclosed in the ring, a screening current J will flow due to the dc Josephson effect. This screening current will induce a magnetic field to make the total magnetic flux inside the ring equal to an integer number of flux quanta Φ_0. The currents through the two sides of the ring will then be $I/2 + J$ and $I/2 - J$. If one of those currents exceeds the critical current I_0 of the junctions, the superconductivity will be broken and a voltage will appear across the junction. The I-V characteristics of the SQUID are shown in figure 2.2(b). This voltage can be measured and will be a function of the screening current and thus of the magnetic flux through the ring. This function will be periodic with the periodicity equal to a flux quantum. For applied magnetic fluxes of integer flux quanta $n\Phi_0$, the screening currents will be zero and the voltage will thus be minimal. For applied magnetic fluxes of $(n + 1/2)\Phi_0$ the screening current and thus the voltage will be maximal.

This can also be seen in figure 2.2(b) and the resulting V-Φ_a diagram can be seen in figure 2.2(c).

As can be seen in figure 2.2(c), the SQUID is the most sensitive to flux changes in the steep parts. That is why the steepest point is used to measure. The SQUID can be locked with a Flux Locked Loop (FLL) around such a steep point, which then becomes the working point. This way the SQUID can measure tiny flux changes as changes in voltage, and keep the working point locked with feedback.

In the LC SQUID thermometer the flux Φ_a is provided by the SQUID input coil. The input coil of the SQUID we use has an inductance of 1 μH and is placed in series with the LC resonator (figure 2.1(b)). This way the current generated inside the resonator also flows through the input coil of the SQUID, converting the signal from current to flux to voltage.

2.3 Quality factor

The coupling between the metal foil whose temperature we want to measure and the inductor will be sufficient when the Q factor is dominated by the dissipation through the metal foil. To be sure that the foil dominates the Q factor, we measure the Q factor of the resonator with and without the foil coupled to the inductor. Here we aim to achieve a high Q factor of at least 1000 without the foil and a relatively much lower Q factor with the foil. This can be achieved by minimizing the contribution of all other Q factor limiting sources such as the capacitor, surrounding metal and the SQUID.

There are two common ways to define the Q factor, which are slightly different, but converge to the same values for larger Q factors. One way is to look at the frequency-to-bandwidth ratio, as shown in formula 2.1 [7].

$$Q = \frac{\omega_r}{\Delta\omega} \tag{2.1}$$

Here ω_r is the angular resonance frequency of the resonator and $\Delta\omega$ is the angular Full Width Half Maximum (FWHM), which is the bandwidth over which the power is greater than half the power at the resonance frequency. Keep in mind here that the power $P = \frac{V^2}{R}$ with V the voltage and R the resistance, and we will be measuring the voltage. So if we want to determine the Q factor from a measurement of the SQUID voltage we will have to look at the bandwidth at $\frac{1}{\sqrt{2}}$ of the voltage at resonance, because $P \sim V^2$.

The second definition for the Q factor is the ratio of the energy stored to the energy dissipated in the resonator by damping processes per cycle [8]. This definition is shown in equation 2.2, and also gives more insight into why the metal foil has an effect on the Q factor. The magnetic field produced by the inductor passes through the metal foil, which dissipates energy through the electrons in the foil. This metal foil-inductor combination can be modelled as a transformer (figure 2.1(b)). If the coupling coefficient between the foil and the inductor is sufficiently high and the foil dominates the Q factor, then according to the fluctuation-dissipation theorem the Johnson noise will be able to induce a current in the inductor which can then be measured with the SQUID [9].

$$Q = \frac{P_{stored}}{P_{dissipated}} = \frac{XI^2}{RI^2} = \frac{\omega_r L}{R} \tag{2.2}$$

In the equation above, $P_{stored/dissipated}$ is the power stored or dissipated in the circuit, X is the reactance of the inductor or capacitor at resonance, I is the current and R is the series resistance. This leads us to an expression for the Q factor in terms of the resonance frequency of the LC resonator ω_r, the inductance of the coil L and the resistance in the LC circuit R.

Chapter 3

The LC resonator

An important part of the thermometer is the LC circuit. To be able to measure the thermal noise in the metal foil, the coupling between the foil and the inductor should be sufficiently high. The thermal agitation of the electrons in the foil induces a small Johnson noise current. This noise current then induces a magnetic field, which in turn induces a noise current in the inductor. This noise current is largest at the resonance frequency of the LC resonator and can then be measured by the SQUID.

Since the Q factor is a measure for how well a resonator can do this amplification, we aim to achieve a sufficiently high Q factor for the resonator. Here we aim for a Q factor of at least 1000 for the resonator without the foil. To best pick up the noise current of the metal foil, we aim for a high coupling between the inductor and the foil. The fluctuation-dissipation theorem predicts that dissipation of energy and the fluctuation of energy are related. This means that if energy is dissipated through the metal foil, Johnson noise from the foil will be induced in the coil. In order to do thermometry, those fluctuations induced in the coil should be larger than the thermal fluctuations of the LC resonator and SQUID, which have a higher temperature than the foil. According to the fluctuation-dissipation theorem, the fluctuations induced in the coil due to the Johnson noise of the foil will be larger if more energy is dissipated through the metal foil. More dissipated energy results in a lower Q factor, which is why we aim for a significant decrease in Q factor when the metal foil is coupled to the resonator, compared with the case without the metal foil.

The Johnson noise of two noise sources at different temperatures can be quadratically added. The total Johnson noise then becomes $4k_BT_1R_1 + 4k_BT_2R_2$, and the Q factor is determined by the total effective resistance $R_1 + R_2$. This means that if the Q factor decreases with a factor

10 when the foil is applied, the effective resistance R_1 of the foil is 9 times larger than the effective resistance R_2 of the other noise source. If the foil is 9 times colder than the other noise source, the noise sources will contribute equally to the total Johnson noise. This means a decrease in Q factor of one order of magnitude will be sufficient. The decrease should not be too big, because we also want the circuit to keep the ability to resonate well enough so that the SQUID can measure the signal.

It is also important that the LC circuit, which has a higher temperature than the foil, produces little Johnson noise itself. An ideal inductor and capacitor will not produce Johnson noise, so to achieve this the circuit resistance should be kept as low as possible. This is done by using superconducting niobium for the inductor and capacitor, and by keeping normal metals away from the vicinity of the coil.

In this chapter, section 3.1 will show the results for the resonator without the metal foil coupled to the inductor and section 3.2 with the metal foil coupled to the inductor.

3.1 Making and testing the resonator without foil

In this section the methods used to measure the Q factor of the LC resonator are explained and the results are given. This is done without the metal foil coupled to the inductor, to be able to determine the change in Q factor and thus the coupling to the metal foil when we do apply the foil in section 3.2. In this chapter the resonator is used without the SQUID.

3.1.1 AC sweep at 4 K to test the Q factor

The Q factor and the coupling between the metal foil and the inductor are tested with a dipstick experiment. In the dipstick experiment the circuit is mounted to the end of a dipstick, which can be submerged in a cryogenic vessel filled with liquid helium. This way the circuit can be cooled to 4.2 K, which is needed to make sure the niobium coil is superconducting. Niobium becomes superconducting below 9.3 K. The dipstick experiment is quick, which makes it ideal for testing the resonator.

To allow the resonator to build up energy at the resonance frequency, high impedances are used to enclose the circuit (figure 3.1). The high impedances are a 1 MΩ resistor $R1$ and a $\sim$1 pF capacitor $C2$ consisting of two parallel wires. The legs of the $R1$ resistor also have an estimated 1 pF capacitance. The inductor used is a 270 μH coil made with niobium wire wound around PEEK. The coil is isolated from the metal of the dipstick

Version of June 19, 2020– Created June 19, 2020 - 18:48

with a niobium foil and plastic separator to minimize unwanted energy dissipation through the metal of the dipstick. The capacitor C is varied throughout the experiment, because the initial 2 nF capacitor used was thought to be a source of dissipation. The other capacitors used are a 18 pF niobium plate capacitor and the inductor's self capacitance. Figure 3.2 shows the coil and the niobium plate capacitor. In the dipstick experiment a Zurich Instruments (ZI) Lock-in Amplifier was used to do an AC frequency sweep and acquire the data. The data is then analysed using the Python `scipy` and `numpy` packages.

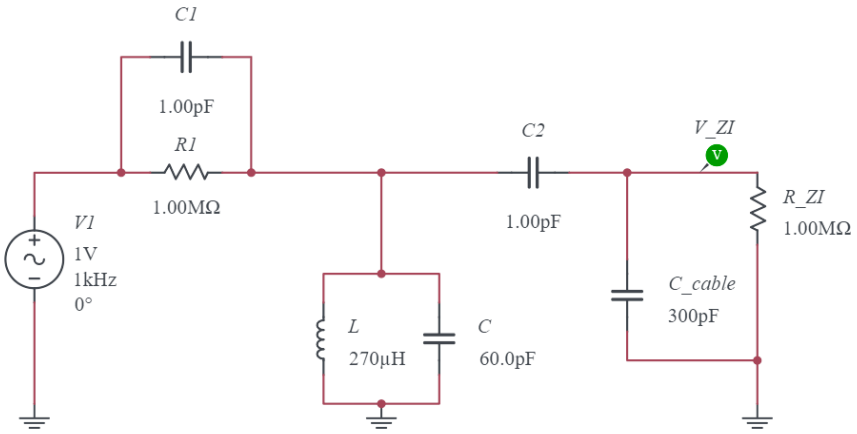

Figure 3.1: *Schematic view of the dipstick experiment. The AC voltage source and green voltage probe are controlled by a ZI Lock-in Amplifier. The resistance of the ZI Amplifier is set to 1 MΩ, and the ∼3 m long coaxial cable is shown as having a capacitance of 300 pF. The LC resonator is blocked in between the high impedances of R1 and C2, allowing it to resonate energy.*

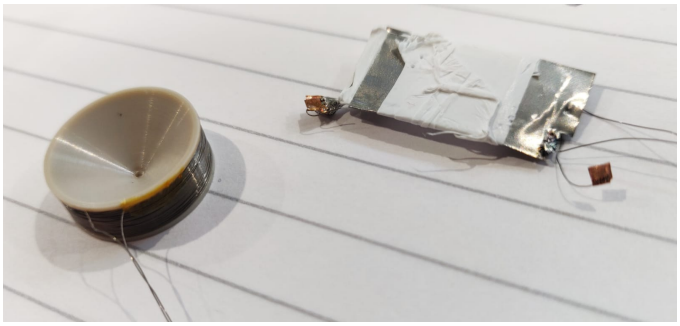

Figure 3.2: *Picture of the 270 µH niobium wire coil and the 18 pF niobium plate capacitor. The two wires leaving the coil are wound together to form a twisted pair, to improve rejection of external electromagnetic interference.*

We will now look at the data sets for the three different capacitors, without a metal foil coupled to the inductor. If we look at the Nyquist plot of the data in figure 3.3, we can see a clear background offset. This background is assumed to be caused by the capacitor and the two different paths the current can flow to. In order to improve the fit, this background is removed, as can also be seen in figure 3.3. This is done with a rotation and translation in the complex domain.

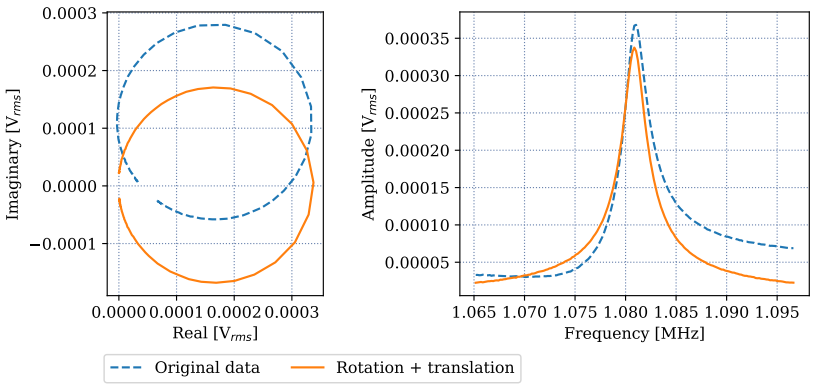

Figure 3.3: *Data of the circuit as in figure 3.1 with a niobium plate capacitor of 18 pF. The blue dashed line represents the original data, and the orange solid line the data with the background removed. The left plot shows the data plotted in the complex domain and the right plot shows the amplitude in V_{rms} as function of the frequency in MHz.*

After the background is removed, the shape of the resonance peak resembles a Lorentzian. This can typically be expected for the resonance peak of a driven underdamped harmonic oscillator. The fitted transfer function is shown in equation 3.1. In appendix I the derivation of the transfer function is given and we show that the fitted transfer function is equivalent to the square root of the Lorentzian.

$$V(\omega) = A \cdot \left| \frac{i\frac{\omega}{\omega_0^2} + \tau}{1 - (\frac{\omega}{\omega_0})^2 + i\omega\tau} \right| + V_0 \tag{3.1}$$

Equation 3.1 shows the transfer function for an RLC series circuit, where we model the circuit resistance R placed after the inductor. Here we fit $\omega_0 = \frac{1}{\sqrt{LC}}$ for the resonance frequency, $\tau = RC$ for the RC time and A and V_0 are parameters to tune the amplitude and offset respectively. Equation 2.2 can then be used to calculate the Q factor. A fit made with this function is shown in figure 3.4.

Version of June 19, 2020– Created June 19, 2020 - 18:48

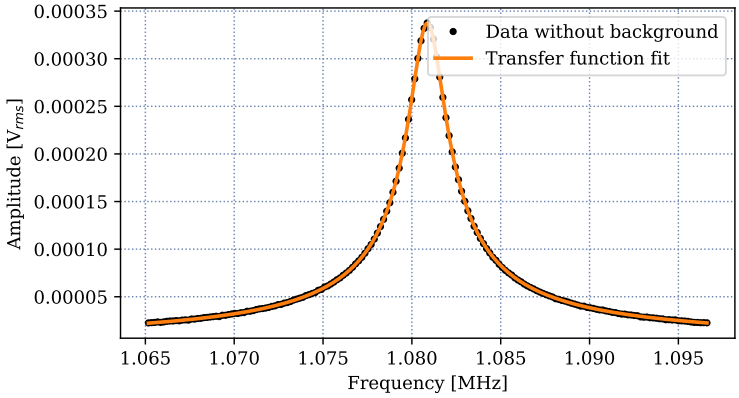

Figure 3.4: *In this figure the black dots represent the data from figure 3.3 with the background removed. The orange line is the Transfer function fit. The y axis shows the amplitude in V_{rms} and the x axis the frequency in MHz.*

Using this procedure to analyse the data, the following Q factors were found for the three capacitances: a Q factor of 776 ± 5 for the 2 nF capacitor, 519 ± 4 for the 18 pF niobium plate capacitor and 442 ± 3 for the 61 pF self capacitance of the coil. The resonance frequencies and RC times are shown in table 3.1. With the resonance frequencies and known capacitances of 2 nF and 18 pF, the inductance can be confirmed to be 270 ± 5 μH and the self capacitance to be 61 ± 2 pF.

Table 3.1: *Results for different capacitances used. The resonance frequency f_r and RC time τ are determined through a fit. The errors are calculated from the fit error and statistical error. Note that the self capacitance of 61 pF was also present in the 2 nF and 18 pF experiments, and can be added to the capacitance since parallel capacitances add.*

Capacitance	**Q factor**	f_r **[MHz]**	τ **[ps]**
2 nF (+61 pF)	776 ± 5	0.216957 ± 0.000003	946 ± 6
18 pF (+61 pF)	519 ± 4	1.080870 ± 0.000005	284 ± 2
61 pF	442 ± 3	1.2327 ± 0.0001	286 ± 2

We expected to achieve a Q factor of at least 1000 with this setup, so the measured Q factors are all lower than expected. This means that the energy must be leaking out of the circuit somewhere. It is also remarkable that the Q factor for the self capacitance is the lowest, while in that experiment there was no separate capacitor to dissipate energy. If the capacitor was the main source of dissipation one would expect the experiment

without the extra capacitor to have the highest Q factor. This means that the capacitor was not the main source of dissipation and that something else is going on. From table 3.1 it can be observed that the Q factor got lower as the resonance frequency got higher. This means there must be a frequency dependent component in the circuit which dissipates more energy for higher frequencies, as the capacitor was the only thing that was changed throughout the three experiments. To find a possible cause for this and improve the Q factor, the circuit was simulated.

3.1.2 Simulating the dipstick circuit

To better understand the circuit and find possible sources of dissipation, the circuit is simulated using National Instruments' online circuit simulator ([10]). This simulator can also be used to try to reproduce the data from table 3.1, and to formulate a hypothesis for the next experiments.

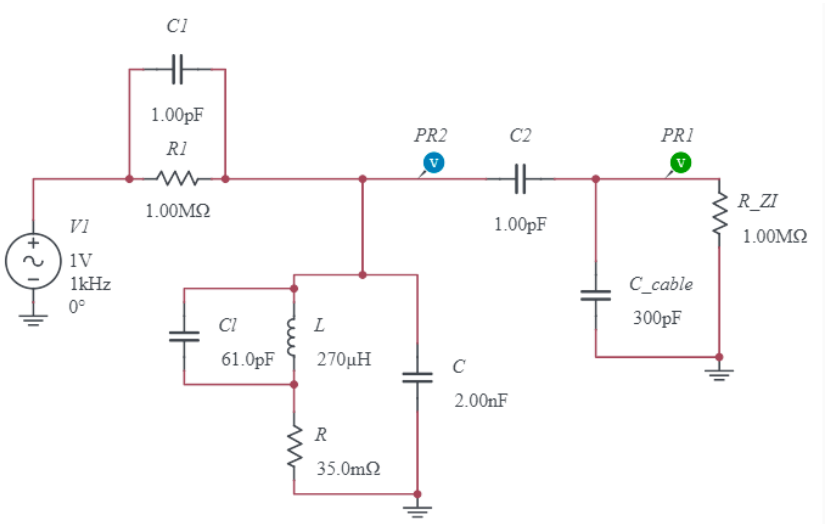

Figure 3.5: *Schematic view of the circuit that was simulated using National Instruments' online circuit simulator ([10]). Here L is the inductor, Cl the self capacitance of the inductor, C the capacitor and R the simulated circuit resistance to account for energy losses in the circuit. The blue and green probes measure the voltages inside the resonator and in the ZI respectively.*

The simulated circuit is shown in figure 3.5. Here the 1 MΩ resistor R1 is simulated with an additional parallel capacitance C1 of 1 pF to take into account the parasitic capacitance of its wires. A perfect capacitor or inductor does not lose energy. Real capacitors and inductors always have

Version of June 19, 2020– Created June 19, 2020 - 18:48

a little bit of energy loss, which can be simulated by placing a small resistor in series behind them. For the losses in the resonator part of the circuit we combine those resistors to a total resistance R, placed between the inductor and capacitor. The very small losses of the C1 and C2 capacitances are ignored in this simulation.

An AC sweep was simulated, which showed that removing the 1 MΩ R1 resistance results in a higher Q factor. This makes sense if one looks at the combined impedance of R1 and C1, which we will call Z_L:

$$|Z_L| = \left|\frac{1}{\frac{1}{R_1} + i\omega C_1}\right| = \frac{1}{\sqrt{1 + (10^{-6}\omega)^2}} 10^6 \tag{3.2}$$

For resonance frequencies higher than $f = \frac{10^6}{2\pi} \approx 160$ kHz, the impedance of the 1 pF capacitance will become lower than the R1 impedance, allowing the energy resonating in the circuit to leak out. The higher the resonance frequency, the lower Z_L will be, and the more energy will leak out. This explains why the Q factor got lower as the resonance frequency got higher. This problem can be easily fixed by taking out the R1 resistor, leaving only the C1 capacitance of the parallel wires.

To estimate the effect this will have on the Q factor, a simulation experiment can be done. The circuit resistance R is chosen such that without the 1 MΩ R1, the Q factor is ∼10.000. The 1 MΩ R1 is then put back, so the difference can be seen. This is done for the 2 nF capacitor. Because the resonance frequency of 217 kHz was bigger than the estimated boundary of 160 kHz, we should see an effect. Also note that this frequency dependent effect will be larger for the higher resonance frequencies of the 18 pF capacitor and self capacitance resonators.

The results of this simulation are shown in figure 3.6. Figure 3.6a shows the resonance peak of the circuit with the 1 MΩ resistor and figure 3.6b shows the resonance peak of the circuit without the 1 MΩ resistor. The resonance peak gets visibly sharper when the resistor is removed and with formula 2.1 quick estimations of the Q factor can be done. Those calculations show that when the 1 MΩ resistor is removed, the Q factor increases from 2.000 to 9.300.

These are promising results, as it means that we likely found the source of energy leaking out and can achieve a high Q factor with this solution. The difference between the simulated voltage inside the resonator (the blue line) and the simulated measured voltage (the green line) is also worth noting. The blue line shows a voltage of a factor 100 higher than the green line. This implies that the voltage inside the resonator is much higher than what we measure with the ZI. This is an effect that can be at-

tributed to the fact that the impedance of the 1 pF coupling capacitor is much higher than the impedance of the 300 pF cable capacitance.

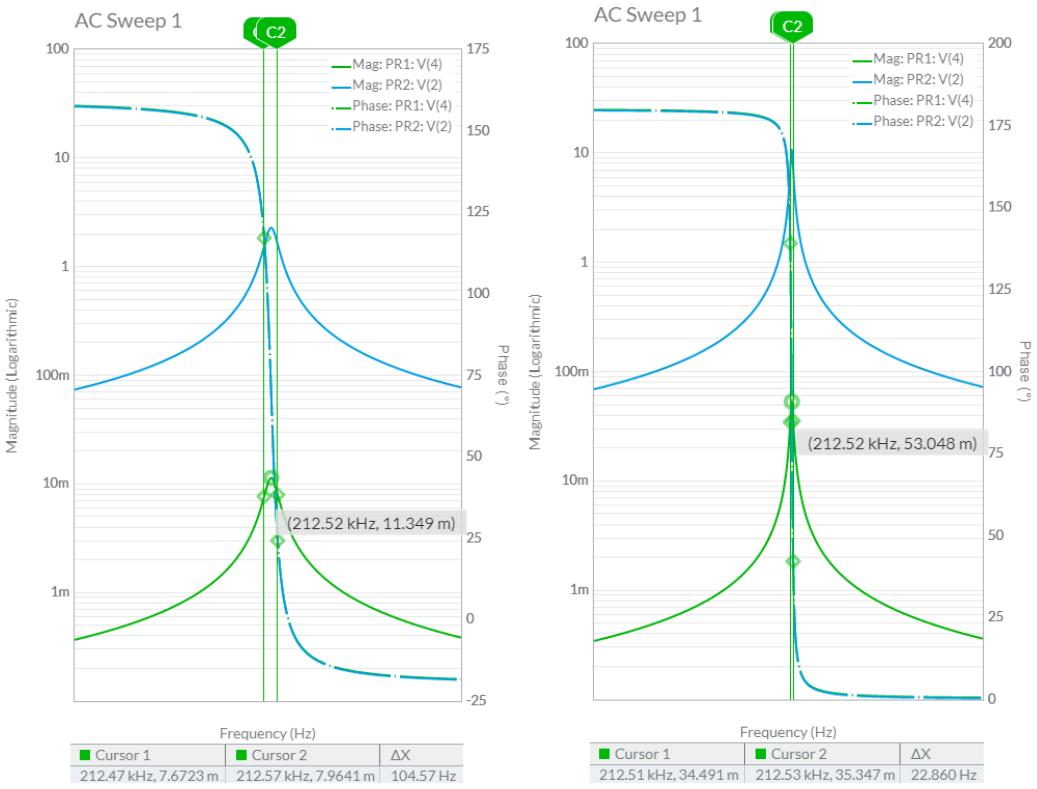

(a) *With the 1 MΩ resistor* ***(b)*** *Without the 1 MΩ resistor*

Figure 3.6: *Simulations to test the effect of the R1 resistor on the Q factor. (a) shows a simulation of the circuit shown in figure 3.5 and (b) shows a simulation of the same circuit with R1 cut out. The blue line represents the simulated voltage at the blue probe in figure 3.5, inside the resonator, and the green line the simulated voltage at the green probe, measured by the ZI. The labels near the green peaks show the resonance frequency and simulated peak amplitude and the ΔX under the figure shows the FWHM. With formula 2.1 a quick estimate of the Q factor can be done, which gives 2000 for (a) and 9300 for (b).*

With equation 3.2 the Q factors found in table 3.1 can be corrected. This gives a Q factor of 1313 ± 8 for the 2 nF capacitor, 3550 ± 30 for the 18 pF niobium plate capacitor and 3450 ± 20 for the 61 pF self capacitance of the coil.

The resonator with the 270 μH inductor and its 61 pF self capacitance as capacitor was tested again without the 1 MΩ R1 resistor. This gave a Q factor of 3361 ± 9, which agrees with the corrected value and is a good

improvement of the earlier found 442 $\pm$ 3. This shows that the 1 MΩ resistor was indeed the limiting factor for the measured Q. With this high Q factor achieved we can now look at the coupling that can be achieved between the metal foil and the inductor.

3.2 Testing the inductor-foil coupling

To get the best coupling, we need as much of the coil's magnetic field as possible to pass through the foil. The best way to do this would be to put the foil inside the coil, but we cannot do this because the coil has a solid center. The next best thing is to completely cover the center of the coil with foil. We will do two experiments: one where only the bottom of the coil is covered by the metal foil and one where both the bottom and top of the coil are covered by bending the foil around the coil.

3.2.1 Results

The two experiments are done with the same setup as the last experiment from chapter 3 where the 1 MΩ resistor was removed. This way the results can be compared to the experiment without the metal foil. A 60 μm thick silver foil is applied to the inductor by securing it with teflon tape. The results are shown in table 3.2.

Table 3.2: *Results for testing the inductor-foil coupling. The resonance frequency f_r and RC time τ are determined through a fit. The errors are calculated from the fit error and statistical error. The capacitor used for the resonator is the self capacitance. The applied metal foil is a silver foil of 60 μm thick.*

Metal foil	**Q factor**	f_r **[MHz]**	τ **[ps]**
none	3361 $\pm$ 9	1.2261 $\pm$ 0.0001	38.7 $\pm$ 0.1
only bottom	688 $\pm$ 2	1.4079 $\pm$ 0.0002	164.3 $\pm$ 0.4
bottom and top	377 $\pm$ 3	1.6687 $\pm$ 0.0001	253 $\pm$ 2

Table 3.2 shows a significant decrease in Q factor when the metal foil is applied. This is a good result, because it means energy is dissipating through the metal foil and we have achieved a good coupling. By applying the foil to both sides of the coil, an even better coupling could be achieved. The resonance frequency shifts significantly when the foil is applied. This is because the effective inductance of the coil becomes lower when the coil is coupled with the foil, as will be derived in section 3.2.3.

Version of June 19, 2020– Created June 19, 2020 - 18:48

A better coupling between the foil and the coil results in a lower Q factor. This means that in order to gain a larger thermal noise signal inside the inductor, we have to sacrifice a certain amount of amplification of this signal. A better coupling with the foil induces a larger noise signal, but the signal is also lost more easily through the foil. To be able to accurately determine the best coupling for our LC SQUID thermometer, we will have to look at the circuit with the SQUID. In chapter 4 a simulation will be done to determine which inductor-foil coupling produces the largest thermal noise current in the SQUID.

3.2.2 A simulation to determine coupling parameters

To be able to decide which type of application of the foil is the best for our thermometer, we again perform a simulation with National Instruments' online circuit simulator ([10]). In this section, a simulation of the circuit shown in figure 3.7 is done. The inductance of the coil is 270 μH and the self capacitance is 61 pF. The value of the simulated resistor R can be computed to be 620 mΩ through formula 2.2, by inserting the values of table 3.2. Testing this value in the simulation without the metal foil indeed gives a Q factor of about 3300. The only parameters left to explore are the coupling coefficient k, the inductance of the foil and the resistance of the foil. If we know those parameters, we can simulate the circuit with the SQUID placed in series to determine what we need for the thermometer circuit.

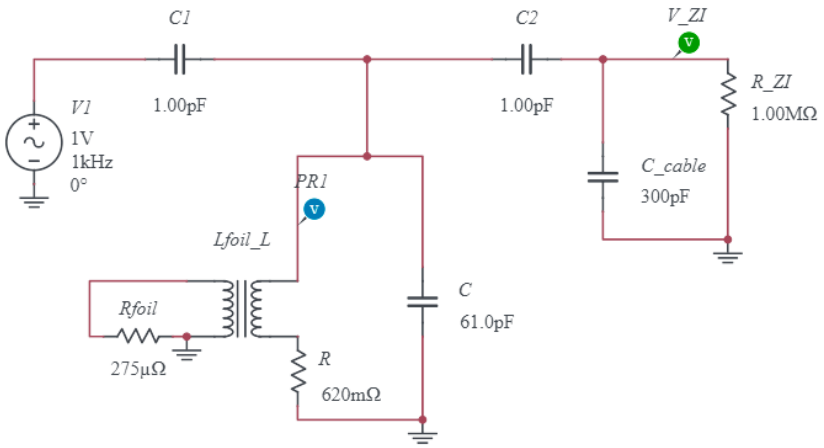

Figure 3.7: *Schematic view of the dipstick circuit that was simulated. The blue and green probes measure the voltages inside the resonator and in the ZI. The inductor and coupled metal foil are simulated as a transformer, L_{foil}_L.*

After varying the different parameters we find that for values of $\omega_r L_{foil} \gg R_{foil}$ the foil affects the peak frequency. This is independent of the coupling coefficient. Around values of $\omega_r L_{foil} = R_{foil}$ the peak shifts from the initial resonance frequency of 1.23 MHz to a new higher resonance frequency, just as was observed in the experimental data when the foil was applied. This means that at resonance the foil's inductor impedance $\omega_r L_{foil}$ should be larger than the foil's resistance R_{foil}. In this transition to the higher resonance frequency the peak has a drastically lower Q factor. Once the peak has transitioned to its new resonance frequency, the R_{foil} and L_{foil} only affect the Q factor of the simulated peak. The coupling coefficient then determines the resonance frequency.

The coupling coefficient can thus be determined through the observed resonance frequencies. This way we find a coupling of $k = 0.50 \pm 0.01$ for the single layer of foil and a coupling of $k = 0.69 \pm 0.01$ for the situation where both the top and bottom of the coil are covered. After this there are two parameters left, R_{foil} and L_{foil}. The ratio of those parameters determines the Q factor and the magnitudes of the values determine the magnitude of the signal. The exact magnitude of the signal is hard to simulate, because it depends on the geometry of the foil and the distance of the foil to the coil. To be able to simulate the LC SQUID circuit we only need the ratio of R_{foil} and L_{foil}, because we are only interested in the ratio between the resonator coil current and the SQUID input coil current and not the exact magnitudes of the currents. For the single layer of foil, a ratio of $\frac{\omega L}{R} = 310$ gives a Q factor of $\sim$690. For the foil on both sides $\frac{\omega L}{R} = 415$ gives a Q factor of $\sim$380. Hence we may conclude that it is indeed possible to see the Q factor decrease with a factor of 10 due to the dissipation in the foil.

3.2.3 Analytical treatment of the coupling coefficient

The coupling coefficient can also be analysed through a theoretical derivation. Here we model the coupled inductor and foil as a transformer where the inductance of the foil is short-circuited. Basic induction equations will then give:

$$\begin{cases} U = i\omega IL + i\omega MI_f \\ U_f = i\omega I_f L_f + i\omega MI = 0 \end{cases} \tag{3.3}$$

Here U represents the voltage over the inductor L, I the current through the inductor and M the mutual inductance of the coil and foil. The subscript f indicates that the respective variable is of the foil side of the trans-

Version of June 19, 2020– Created June 19, 2020 - 18:48

former. U_f is equal to 0 because the circuit of the foil can be seen as short-circuited. Through this equation we then find:

$$I_f = -\frac{M}{L_f} I \tag{3.4}$$

Inserting this into the other equation, we find:

$$U = i\omega\Big(L - \frac{M^2}{L_f}\Big) I = i\omega L(1 - k^2) I \tag{3.5}$$

Where in the second part we used that the mutual inductance is defined as $M = k\sqrt{L\,L_f}$. From equation 3.5, we can see that the effective inductance of the inductor coupled with the foil becomes $L_{eff} = (1 - k^2)L$. Rewriting this and using that k is positive gives:

$$k = \sqrt{1 - \frac{L_{eff}}{L}} = \sqrt{1 - \frac{\omega_r^2}{\omega_0^2}} \tag{3.6}$$

Here ω_0 is the resonance frequency of the resonator when coupled with the foil and ω_r the resonance frequency of the resonator without the foil. In the second part we used that the effective inductance can be calculated from the measured resonance frequency with $L_{eff} = \frac{1}{\omega_0^2 C}$. The self capacitance C that was used as capacitor stayed the same and thus cancels out. By plugging the values from table 3.2 into this equation, we find coupling coefficients of 0.49 and 0.68 for the coil with the single foil and foil on both sides respectively. This matches our simulated result from section 3.2.2.

Version of June 19, 2020– Created June 19, 2020 - 18:48

Chapter 4

Testing the SQUID thermometer

In this chapter the thermometer will be completed by placing the SQUID input coil in series with the resonator, as shown in figure 2.1(b). The SQUID used is a two stage Magnicon XL SQUID, which has a 1 μH input coil. Calculations to determine the signal we can expect are done in section 4.1. The experimental setup and results are given in section 4.2.

The main experimental unknown at the outset of the experiment was whether or not the bandwidth of the SQUID feedback electronics would allow measuring the noise signals at 1 MHz. This could also have implications for a future attempt to measure shotnoise in the STM experiments in the Allan group [11] using SQUIDs and LC resonators at approximately 10 mK. The bandwidth of the SQUID feedback is calculated in section 4.3.

4.1 Theoretical results

The final LC resonator with the metal foil coupled to the inductor that was created in chapter 3 was the 270 μH niobium wire inductor with its 61 pF self capacitance. To create the thermometer we want to place the SQUID in series with the resonator so that the current can flow through the 1 μH SQUID input coil. However, we cannot place the SQUID in series with the self capacitance, as this is a capacitance between the wires wound around the coil. An extra capacitor will thus be needed. For this we aim to use a niobium plate capacitor to maintain a high Q factor. The expected signal in the resonator coil and the SQUID noise are calculated in section 4.1.1. To calculate how high the capacitance should be in order to have a fair amount of the noise current in the LC resonator running through the SQUID inductance, we again simulate the circuit in section 4.1.2.

4.1.1 Theoretical calculation of signal in the resonator

In order to do thermometry we need to be able to measure the Johnson noise generated by the metal foil. To determine the signal that can be expected and the capacitor that is needed, we calculate the noise signal that is generated in the resonator coil by the Johnson noise in the metal foil. This signal needs to be larger than the SQUID noise, which is typically a few $\mu\Phi_0/\sqrt{\text{Hz}}$ for dc SQUIDs [6]. The SQUID we use has an input coil with inductance 1 μH, which means 1 $\mu\Phi_0/\sqrt{\text{Hz}}$ noise is equivalent to a noise current in the input coil of $I_n = \frac{1\mu\Phi_0}{L_{squid}} \approx 2 \cdot 10^{-15}\text{A}/\sqrt{\text{Hz}}$.

The Johnson noise U_J at temperature T in an electrical component with a resistance R is a white noise spectrum given by the following equation:

$$U_J = \sqrt{4k_BTR} \tag{4.1}$$

Here U_J has dimensions of $\text{V}/\sqrt{\text{Hz}}$. The root mean square voltage can be calculated by multiplying U_J with the square root of the bandwidth, which in our case is given by $\Delta\omega = \frac{\omega_r}{Q}$ (equation 2.1). To determine the Johnson noise induced in the inductor by the metal foil, the resonator coupled with the foil is approximated as an RLC series circuit. The inductor L is the effective inductance of the circuit and the resistor R the effective resistance. The effective resistance can be calculated with equation 2.2. We can use the following equation to calculate the current per $\sqrt{\text{Hz}}$ in the resonator at resonance due to the Johnson noise in the foil, taking into account that at resonance the impedances with opposite signs $i\omega_r L$ and $\frac{-i}{\omega_r C}$ cancel:

$$I_J = \frac{U_J}{R} = \sqrt{\frac{4k_BT}{R}} = \sqrt{\frac{4k_BTQ}{\omega_r L_{eff}}} = \sqrt{4k_BTQ\omega_r C} \tag{4.2}$$

If we use $L_{eff} = (1 - k^2)L$, which was derived in section 3.2.3, we get the following:

$$I_J = \sqrt{4k_BTQ\sqrt{\frac{C}{(1-k^2)L}}} \tag{4.3}$$

With this formula we find noise signals of $1.4 \cdot 10^{-13}\text{A}/\sqrt{\text{Hz}}$ and $1.2 \cdot 10^{-13}\text{A}/\sqrt{\text{Hz}}$ for the inductor with a single layer of foil and with the foil on both sides respectively. This noise signal was calculated for a temperature of 1 mK and gets larger for higher temperatures, as the noise current scales with $\sqrt{T}$.

Version of June 19, 2020– Created June 19, 2020 - 18:48

The values of $1.4 \cdot 10^{-13}\mathrm{A}/\sqrt{\mathrm{Hz}}$ and $1.2 \cdot 10^{-13}\mathrm{A}/\sqrt{\mathrm{Hz}}$ mean a slightly higher signal may be expected for the inductor coupled with a single layer of foil. This can be explained with the decrease in Q factor. Because of the better coupling between the foil and the inductor the noise signal is induced in the coil more easily, but also dissipated more easily. Alternatively, it may be explained that there is $\frac{1}{2}k_BT$ in this mode but for a higher Q, this energy sits in a smaller bandwidth.

4.1.2 Simulating the circuit

In this section the thermometer circuit is simulated to determine the capacitance needed to get a good signal in the SQUID input coil. The simulated circuit is shown in figure 4.1(a). Here the coupled inductor and metal foil are simulated the same way as in section 3.2. The wires connecting the inductor, capacitor and SQUID input coil are modelled as having a 10 pF capacitance. This is a a rough upper limit, equivalent to 10 cm of a twisted pair. If the capacitance of the wires is lower, there will be more signal in the SQUID input loop and the resonance frequency will be slightly higher. The blue probe measures the current inside the resonator coil and the green probe measures the current inside the input coil of the SQUID.

To determine a design value for the value of the capacitor in the experiment, the ratio of current in the input coil to the current in the resonator coil is measured for different capacitances. The capacitor that will be used is a niobium plate capacitor, which means values of 10-100 pF are realistic. The capacitance in the simulation is varied from 10 pF to 640 pF with a logarithmic distribution. The results for the two different coupling coefficients are shown in figure 4.2, with solid lines. The fraction of current in the input coil increases with the capacitance. For the stronger coupling k=0.69 we find a higher fraction of current in the input coil. The resonance frequencies of the simulated circuits varied from 1.5 MHz to 500 kHz, which are all frequency values within the measurement range of the SQUID and thus not important for the choice of the capacitor C.

The simulated fraction of current in the input coil becomes greater than 1. This means the signal in the SQUID input coil is higher than the signal generated in the resonator coil. Intuitively the maximum possible fraction should be 1, so there could be something missing in the simulation. To simplify the simulation, the transformer part which simulates the foil is replaced with an inductor with a calculated effective inductance of 209 μH and 149 μH for k=0.50 and k=0.69 respectively (figure 4.1(b)). An effective resistance of 2 Ω is simulated to limit the Q factor, which does not

affect the fraction of current in the SQUID coil. The AC voltage source is placed in series with the inductor. Doing the same simulations with this circuit gives a fraction of current in the SQUID input coil which does not exceed 1, and is the same for both effective inductances. This is shown in figure 4.2 with the dotted lines.

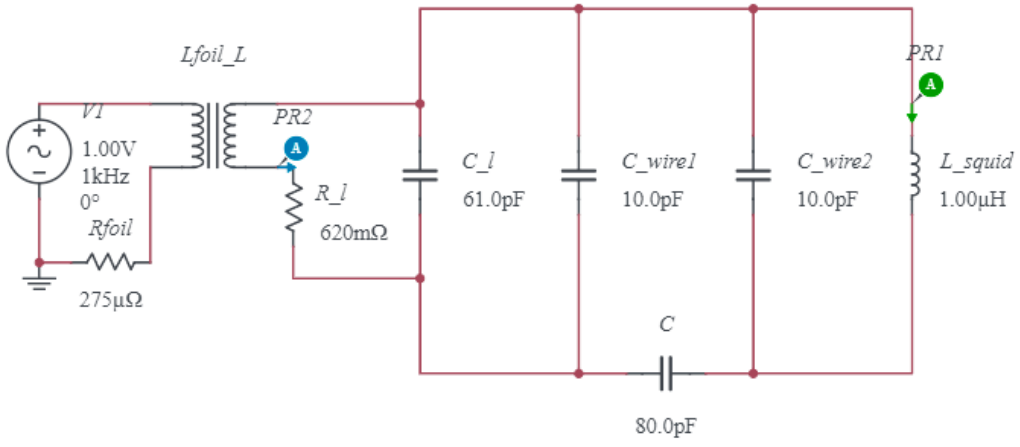

(a)

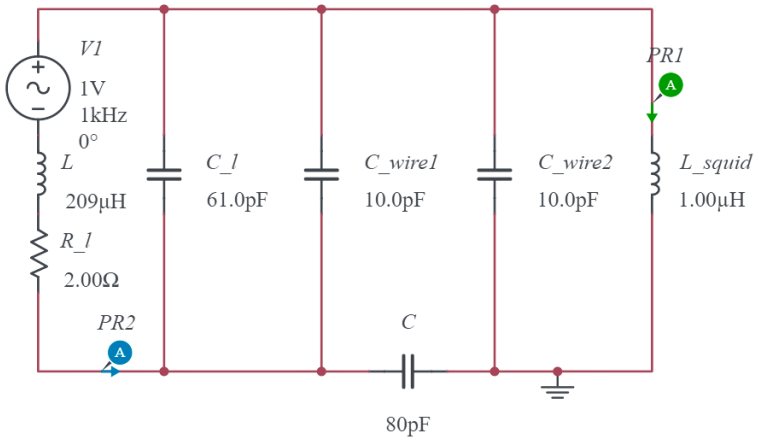

(b)

Figure 4.1: *Schematic views of the thermometer circuits that were simulated using National Instruments' online circuit simulator ([10]). The blue and green probes measure the voltages inside the inductor and in the SQUID input coil L_{squid}. In (a) the inductor and coupled metal foil are simulated as a transformer, $Lfoil\_L$. In (b) the inductor and coupled metal foil are simulated as an effective resistance.*

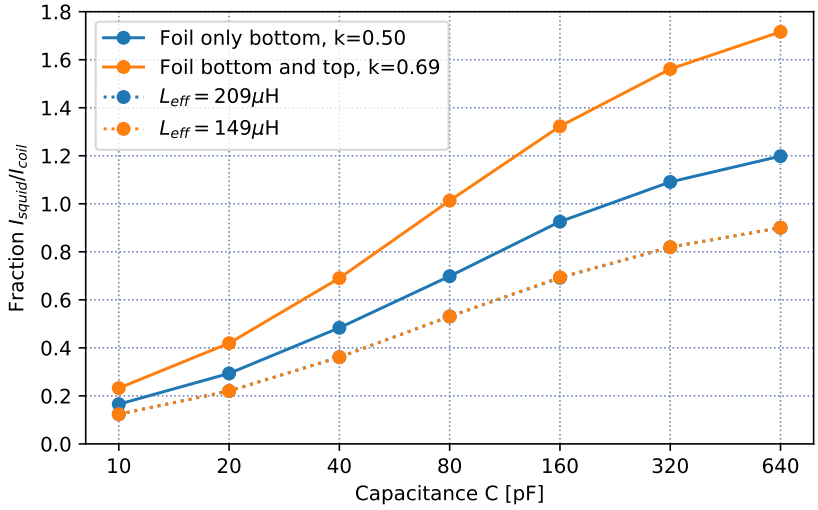

Figure 4.2: *The simulated fraction of current in the squid input over the current in the resonator coil for different values of C. The x axis is a logarithmic scale which shows the capacitance in pF. The solid blue line represents the values for the coil with a single layer of foil and the solid orange line represents the coil with the foil applied to both the top and bottom. The orange and blue dotted lines overlap and show the simulated values for the simplified circuit without the transformer.*

The simplified simulation gives the lowest fractions of current in the SQUID input coil. We will use those values as a lower limit to calculate the minimum signal we can expect in the SQUID input coil. The noise signals calculated in section 4.1.1 in the coil at 1 mK are a factor 50 higher than the estimated SQUID noise. This means that if 20% of the signal in the inductor reaches the SQUID input coil, we should still be able to measure the signal with a signal-to-noise (S-N) ratio of 10. With the simulation results we can thus conclude that a capacitor of 20 pF will be sufficient and if the capacitance is higher the signal will be better. By using multiple layers of niobium foil on top of each other we were able to make a niobium plate capacitor of 80 pF. This means we can expect an S-N ratio of about 40 for the single layer of foil and an S-N of about 30 for the foil on both sides. This, as well as the fact that we are for now working at temperatures larger than 1 mK, is the reason why we choose to only apply the foil to one side of the inductor.

4.2 Experimental results

According to the calculations in section 4.1, the thermometer should be able to measure millikelvin temperatures with an S-N ratio of at least 40. If we increase the temperature, the S-N ratio will get even better. To be able to quickly vary the temperature and check if the surface of the peak changes with the temperature as expected, we place the thermometer on the MC plate and attach the silver foil to the 50 mK plate. There is also a heater on the 50 mK plate, which can be used to increase the temperature of the foil. Existing calibrated thermometers on the 50 mK plate and other plates can be used to determine the temperature. The LC SQUID thermometer is placed in an aluminium box to shield the experiment from surrounding metals and noise. Aluminium becomes superconducting below 1.2 K. This setup can thus be used to test the thermometer for a temperature range of 50 mK - 1 K. A picture of this setup is shown in figure 4.3.

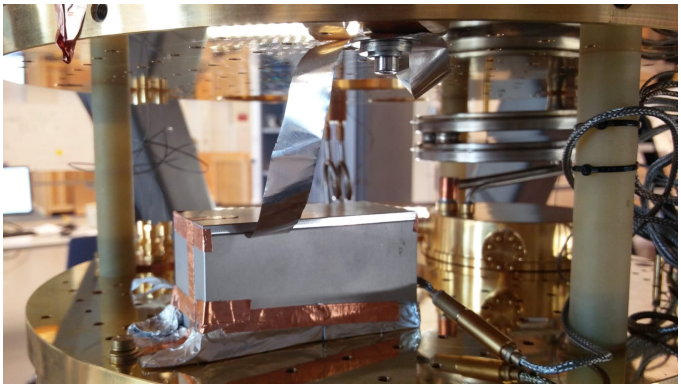

Figure 4.3: *The aluminium box which contains the LC SQUID thermometer. The silver foil is coupled to the inductor inside the box, and exits the box through a thin slit beneath the lid, carved in the box wall. The SQUID electronics exit the box through a hole in the short side on the right.*

The LC thermometer tested consisted of the 270 μH niobium coil coupled with a single layer of 60 μm thick silver foil (k$\approx$0.5) and placed in series with the 80 pF niobium plate capacitor and the 1 μH SQUID input coil (figure 4.4). The voltage output of the SQUID was sent to a ZI lock-in amplifier capable of doing frequency sweeps and analysing the spectrum with an FFT. With the calculations and simulation done in section 4.1, the resonance peak was expected around 910 kHz, with a width of about 2 kHz (Q factor around 500).

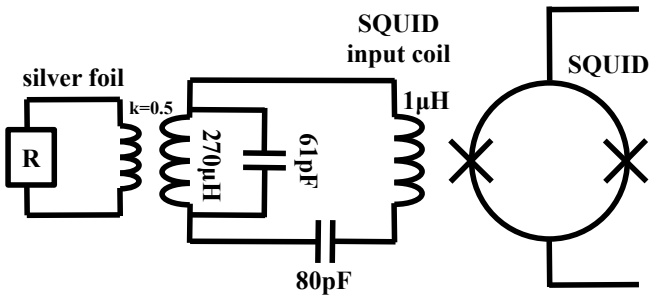

Figure 4.4: *Schematic of the LC SQUID thermometer. The silver foil is inductively coupled to the coil and can therefore be modeled as a resistor in series with an inductor. The foil is coupled to the coil with k=0.5. The 61 pF capacitance is the coil's parasitic capacitance and the 80 pF capacitor is a niobium plate capacitor.*

We initially found a peak with a width of about 20 kHz at 920 kHz with a smaller peak of width 2 kHz at 918 kHz on top of the wider peak. Further measurements showed that the resonance frequency of the wider peak is dependent on the SQUID feedback and SQUID temperature, and shifts significantly if the SQUID feedback settings are changed, i.e. a different Gain Bandwidth Product (GBP) is used for the amplifier in the feedback loop or if a different feedback resistor Rf is used in the conversion of the SQUID voltage to a current in the feedback coil of the SQUID. The data is shown in figure 4.5.

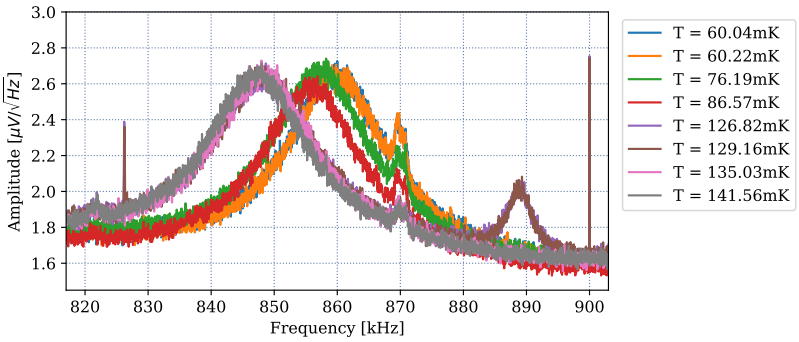

Figure 4.5: *The temperature dependency of the measured wide resonance peak. The legend shows the temperature of the 50 mK plate. The GBP was 4 GHz and the Rf resistance was 10 kΩ*

More smaller peaks were found around 870 kHz and 820 kHz, and the smaller peaks were only visible when on top of the bigger peak. Integrat-

ing the surface of the peaks showed no clear increase when the temperature was increased. In two measurements done right after relocking the FLL another peak can be seen at 890 kHz. This peak could not be reproduced in further measurements. Further research is needed to determine the exact cause of those peaks, which seem to emanate from the SQUID feedback electronics. A clear resonance peak that could be attributed to the thermometer was not found.

4.3 Calculating the SQUID bandwidth

To check if the bandwidth of the SQUID feedback electronics allowed measuring the signal at 1 MHz, the SQUID bandwidth is calculated. If the SQUID bandwidth is too low, this could result in the S-N of the signal being smaller, or the signal not being measured at all. The bandwidth is the 3dB frequency, and depends on the way the SQUID is tuned. The 3dB frequency can be calculated to check if the bandwidth is sufficient to measure frequencies around 1 MHz.

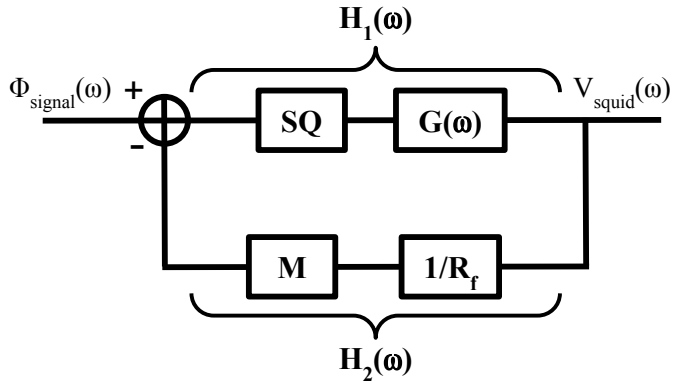

Figure 4.6: *Schematic of the SQUID feedback loop. Negative feedback is used to subtract the output signal $V_{squid}(\omega)$ from the input signal $\Phi_{signal}(\omega)$ via the transfer function $H_2(\omega)$.*

The SQUID feedback is a negative feedback system, where the input signal is the measured flux in the SQUID input coil $\Phi_{signal}(\omega)$ and the output signal is the voltage we measure $V_{squid}(\omega)$. A schematic of the feedback can be seen in figure 4.6. The closed loop transfer function of this feedback system is given by:

$$H(\omega) = \frac{H_1(\omega)}{1 + H_1(\omega)H_2(\omega)} \tag{4.4}$$

The transfer function $H_1(\omega)$ converts the measured flux to a voltage, and consists of the transfer coefficient SQ and the gain $G(\omega)$. SQ converts the measured flux offset to a voltage according to the slope of the working point around which the SQUID is locked with an FLL. The transfer coefficient SQ can be calculated with the following equation:

$$SQ = \frac{\Delta y}{\Delta x} \frac{V_{period}}{G_{Amp}} \tag{4.5}$$

Here $\frac{\Delta y}{\Delta x}$ is the slope of the working point, V_{period} is the voltage in the x direction for one period of the SQUID modulation to scale the x value to one flux quantum and G_{Amp} is the SQUID Amp gain to take the amplification of the voltage value into account. The transfer coefficient SQ is in V/Φ_0.

The gain $G(\omega)$ can be determined from the gain bandwidth product (GBP) with the following equation:

$$G(\omega) = \frac{G_0}{1 + i\frac{G_0\omega}{GBP}} \approx \frac{GBP}{i\omega} \tag{4.6}$$

Here G_0 is a large constant, which allows us to approximate the gain for frequencies $G_0\omega \gg GBP$. We use this approximation for all frequencies smaller than the GBP while it is valid only for frequencies smaller than the GBP but larger than GBP/G0. However the approximation may be used at lower frequencies as well without changing the result found for the closed loop gain. The GBP is in rad/s. This results in the following expression for the transfer function $H_1(\omega)$:

$$H_1(\omega) = SQ \cdot G(\omega) \approx \frac{SQ \cdot GBP}{i\omega} \tag{4.7}$$

The transfer function $H_2(\omega)$ is used to convert the voltage $V_{squid}(\omega)$ to a feedback flux, and consists of two parts: a feedback a feedback resistor R_f to convert the voltage to a current and the mutual inductance M to convert the current to a flux. The mutual inductance M can be determined using the reciprocal of the current needed in the feedback coil to produce one flux quantum, which can be calculated by multiplying V_{period} with the peak-to-peak value of the generator:

$$M = \left(\frac{V_{period} \cdot \text{peak-to-peak}}{1V \cdot 1\Phi_0} \right)^{-1} \tag{4.8}$$

With $H_2 = M/R_f$ the total transfer function of the system can now be written in terms of SQ, M, R_f and the GBP:

Version of June 19, 2020– Created June 19, 2020 - 18:48

$$H(\omega) = \frac{\frac{SQ \cdot GBP}{i\omega}}{1 + \frac{SQ \cdot GBP}{i\omega} \cdot \frac{M}{R_f}} = \frac{R_f/M}{1 + i\omega \frac{R_f}{SQ \cdot GBP \cdot M}} \tag{4.9}$$

From this transfer function we can easily see that the 3dB frequency, and thus the SQUID bandwidth, is given by:

$$f_{3dB} = \frac{SQ \cdot GBP \cdot M}{R_f} \tag{4.10}$$

Here the GBP is in Hz. The values needed to calculate the bandwidth for the run in the dilution refrigerator that was done in section 4.2 are shown in table 4.1. Those values give a bandwidth of $f_{3dB} \approx 8.0$ MHz. This means the SQUID should have been able to measure a resonance peak around 910 kHz, and the absence of the peak is caused by something else.

Table 4.1: *Values needed to determine the SQUID bandwidth from the SQUID tuning in the experiment described in section 4.2*

Property	**Value**	**Property**	**Value**
$\Delta y/\Delta x$	0.15/0.075	**GBP**	4 GHz
V_{period}	0.94 V	**peak-to-peak**	50.12 μA
G_{Amp}	2000	R_f	10 kΩ

Version of June 19, 2020– Created June 19, 2020 - 18:48

Chapter 5

Discussion & conclusions

In this chapter the results of chapters 3 and 4 are discussed and the conclusions are given. Finally some future improvements are given in the outlook.

5.1 The LC resonator

A 270 ± 5 μH niobium wire coil with a self capacitance of 61 ± 2 pF and a 18 pF niobium plate capacitor were used to create an LC resonator with a high Q factor of $\sim$3500. This value was not directly measured, but calculated by correcting the measured Q factor of 519 for the dissipation through the 1 MΩ resistor that was used to enclose the circuit to resonate energy. The same correction for the coil with its self capacitance as capacitor predicted a Q factor of $\sim$3450, where running the experiment with an improved impedance showed a Q factor of 3361 ± 9. This shows that the correction is good and we can thus assume the Q factors for the 18 pF niobium plate capacitor and the 2 nF capacitor to be $\sim$ 3500 and $\sim$ 1300 respectively.

The 80 pF niobium plate capacitor that was used for the thermometer was not individually tested. The assumption was made that the energy dissipation through this capacitor is of the same order as the energy dissipation through the 18 pF capacitor, which means the Q factor of the resonator with this 80 pF capacitor is in the same order of magnitude, $>$1000.

The coupling between the silver foil and the coil is assumed to be constant for different resonance frequencies and different temperatures below 4K. The coupling coefficients found were $k = 0.50 \pm 0.01$ and $k = 0.69 \pm 0.01$ for the coil covered with the foil on one side and on both

sides respectively. If the coupling changes considerably with the temperature or frequency this would complicate the calculations. If the skin depth becomes smaller, the current on the edge of the metal becomes larger which might make for a higher coupling between the metal and the coil. For the values of the conductance of silver at room temperature the skin depth is $\sim$50 μm at 1 MHz. The skin depth is inversely proportional to the square root of the frequency and conductivity. Because at low temperatures the conductivity may very well be 100 times better than at room temperature [12] we assume that the inductance of the coil is strongly affected by the foil and that hence the coupling is quite strong.

5.2 The SQUID thermometer

The simulation of the thermometer circuit to determine the ratio of current in the SQUID input coil to the current generated in the resonator coil. This simulation initially showed ratios bigger than 1 for capacitances $>$80 pF, which means that the simulated current in the input coil is higher than the current in the resonator coil. Because we would expect the maximum ratio to be 1, a second simplified simulation was done which did show a ratio with maximum of 1. To determine which simulation is correct and which parts of the simulation have to be adjusted more research is needed.

With the setup used in chapter 4 a resonance peak with an S-N of at least 40 was expected. The resonance peak was predicted to have a resonance frequency of 910 kHz and width of about 2 kHz. A peak with a resonance frequency which changed when the SQUID feedback settings were changed and a width of about 20 kHz was measured, but no clear temperature dependent resonance peak was seen that could be attributed to the thermometer.

5.3 Outlook

The S-N ratio of the thermometer can be improved by further improving the Q factor of the resonator. To check if the calculation of the Q factor of the current resonator with the 80 pF capacitance is correct, a dipstick experiment could be done with the resonator as was done in chapter 3. The verify if the coupling coefficient is constant for different frequencies the experiment with the foil could also be redone for this resonator. In this experiment the temperature could also be varied with a heater to check if the coupling coefficient remains constant for different temperatures. Lit-

erature research into the skin depth and coupling between a metal foil and inductor can also be done to determine the influence of this on the thermometer.

More research can be done into the cause of the observed 20 kHz wide resonance peak which seemed to emanate from the SQUID feedback electronics. It is important to find the cause of this peak to prevent the unwanted peak from showing up in future experiments. More research can also be done into creating a good simulation for the thermometer circuit, as there are currently two different versions which show different results for the ratio of current in the SQUID input coil.

To check if a resonance peak can be measured with this setup, an additional dipstick experiment could be done with the SQUID in liquid helium at 4.2 K. Instead of coupling the foil to the coil and measuring the Johnson noise, a flux can be sent through a loop placed near the coil to simulate a strong signal.

If the resonance peak of the LC SQUID thermometer can be found in future experiments, the dependence of the surface of the peak on the temperature of the SQUID should be tested to be sure that the SQUID temperature doesn't affect the thermometer. This can be done by independently varying the temperatures of the MC plate to which the SQUID as well as the LC resonator are thermalized, and the 50 mK plate to which the metal foil is thermalized. This will help to make a model of the energy in the LC resonator based on the temperature of the foil which is attached to the 50 mK plate and the SQUID, capacitor and inductor which are thermalized to the MC plate.

Appendix A

Resonance peaks as Lorentzian line shapes

It is not uncommon to assume a resonance peak for a driven underdamped harmonic oscillator takes the shape of a Lorentzian. In this section the transfer function used to fit the Q factor will be derived, and we will prove this function can be approximated as the square root of the Lorentzian function, based on T. Satogata's notes [13].

A.1 Derivation transfer function used to fit

To fit the resonance peak we used the transfer function of the resonator part of the circuit. The transfer function $H(\omega)$ is defined as the output that is measured divided by the input that is put into the circuit. In the dipstick circuit the output is the voltage over the resonator and the input is the current through the resonator. This means that the transfer function is the impedance of the resonator part. For the inductor L and circuit resistance R placed in parallel with the capacitor C, this is:

$$H(\omega) = \frac{1}{\frac{1}{R+i\omega L} + i\omega C} = \frac{R + i\omega L}{1 + i\omega RC - \omega^2 LC} \tag{A.1}$$

If we then substitute the resonance frequency $\omega_0 = \frac{1}{LC}$ and the RC time $\tau = RC$ we get the following:

$$|H(\omega)| = \left| \frac{i\frac{\omega}{\omega_0^2} + \tau}{1 - (\frac{\omega}{\omega_0})^2 + i\omega\tau} \right| \tag{A.2}$$

This was the function that was used to fit the resonance peak.

A.2 Derivation Lorentzian shape of the resonance peak

To show that this is can be approximated to a Lorentzian, we first make the following approximation:

$$|H(\omega)| = \sqrt{\frac{\frac{\omega^2}{\omega_0^4} + \tau^2}{\left(1 - (\frac{\omega}{\omega_0})^2\right)^2 + \omega^2\tau^2}} \approx \frac{\tau}{\sqrt{\omega^2\tau^2 + \left(1 - (\frac{\omega}{\omega_0})^2\right)^2}} \tag{A.3}$$

Here we used the approximation $\frac{\omega^2}{\omega_0^4} \approx 0$ for frequencies around ω_0, because then $\omega^2 \approx \omega_0^2$ and for high resonance frequencies $\omega_0^4 >> \omega_0^2$. We then make a first order Taylor expansion of ω around the resonance frequency ω_0 for the $(\frac{\omega}{\omega_0})^2$ term:

$$\left(\frac{\omega}{\omega_0}\right)^2 = 1 + \frac{2}{\omega_0}(\omega - \omega_0) + \mathcal{O}(\omega^2) \tag{A.4}$$

This gives the following function:

$$|H(\omega)| = \frac{\tau}{\sqrt{\omega^2\tau^2 + \frac{4}{\omega_0^2}(\omega - \omega_0)^2}} \tag{A.5}$$

If we make an approximation of the $\omega^2\tau^2$ term around $\omega = \omega_0$, we get:

$$\omega^2\tau^2 = \omega_0^2\tau^2 + 2\omega_0\tau(\omega - \omega_0) + \mathcal{O}(\omega^2) \tag{A.6}$$

For the high frequency limit the resonance frequency $\omega_0 >> \omega - \omega_0$. This means $\omega^2\tau^2$ can be approximated as $\omega_0^2\tau^2$, where we drop the far smaller first order term. This gives the formula:

$$|H(\omega)| = \frac{\tau}{\sqrt{\omega_0^2\tau^2 + \frac{4}{\omega_0^2}(\omega - \omega_0)^2}} \tag{A.7}$$

The Lorentzian function is defined as:

$$f(\omega) = \frac{1}{\pi\gamma[1 + (\frac{\omega - \omega_0}{\gamma})^2]} \tag{A.8}$$

Version of June 19, 2020– Created June 19, 2020 - 18:48

By rewriting equation A.7 we find:

$$|H(\omega)| = \frac{1}{\sqrt{\omega_0^2\left[1 + \frac{4}{\omega_0^4\tau^2}(\omega - \omega_0)^2\right]}} = \frac{1}{\sqrt{\omega_0^2\left[1 + (\frac{\omega-\omega_0}{\gamma})^2\right]}} \tag{A.9}$$

Here we used $\gamma = \frac{\omega_0^2\tau}{2}$. This equation is mathematically identical to the square root of the Lorentzian function. The only difference is a constant $\frac{1}{\sqrt{\frac{\pi\tau}{2}}}$ which should be multiplied with $|H(\omega)|$ to get the expression from equation A.8.

Acknowledgements

I want to thank Tjerk for being a very active supervisor, and for all the help and feedback given to me during my project. When I had to stay at home for 3 months due to the COVID-19 pandemic (mid march - mid june) I still felt included and connected to the group due to daily phone calls and the ability to carry out my experiments online. I would also like to thank both my daily supervisors Freek and Tim, and the rest of the Oosterkamp group for the usefull and fun discussions and the great atmosphere. I would like to thank Tim especially for physically setting up my experiments during the pandemic. I learned a lot during my time in the Oosterkamp group and really enjoyed doing this project.

I want to thank the FMD and the ELD for always being there to help with small tasks. Finally I would like to thank everyone else who helped me with my project, and everyone who helped keep everyone safe during these crazy times.

Bibliography

[1] A. Bassi, K. Lochan, S. Satin, T. P. Singh, and H. Ulbricht, *Models of wave-function collapse, underlying theories, and experimental tests*, Reviews of Modern Physics **85**, 471 (2013).

[2] A. Vinante, M. Bahrami, A. Bassi, O. Usenko, G. Wijts, and T. Oosterkamp, *Upper bounds on spontaneous wave-function collapse models using millikelvin-cooled nanocantilevers*, Physical review letters **116**, 090402 (2016).

[3] M. d. Wit et al., *Advances in SQUID-detected magnetic resonance force microscopy*, PhD thesis, 2019.

[4] B. HDL, *SRD1000 measurement systems*.

[5] J. Engert, J. Beyer, D. Drung, A. Kirste, D. Heyer, A. Fleischmann, C. Enss, and H. Barthelmess, *Practical noise thermometers for low temperatures*, in *Journal of Physics: Conference Series*, volume 150, page 012012, IOP Publishing, 2009.

[6] J. Clarke and A. I. Braginski, *The SQUID handbook. Vol. 1, Fundamentals and technology of SQUIDs and SQUID systems*, Wiley-VCH, 2004.

[7] E. I. Green, *The story of Q*, American Scientist **43**, 584 (1955).

[8] T. Kuphaldt, *Lessons In Electric Circuits, Volume II–AC*, 2007.

[9] H. Nyquist, *Thermal agitation of electric charge in conductors*, Physical review **32**, 110 (1928).

[10] *Multisim Live Online Circuit Simulator*, `https://www.multisim.com/`, Accessed: march/april 2020.

[11] K. Bastiaans, T. Benschop, D. Chatzopoulos, D. Cho, Q. Dong, Y. Jin, and M. Allan, *Amplifier for scanning tunneling microscopy at MHz frequencies*, Review of Scientific Instruments **89**, 093709 (2018).

[12] R. A. Matula, *Electrical resistivity of copper, gold, palladium, and silver*, Journal of Physical and Chemical Reference Data **8**, 1147 (1979).

[13] T. Satogata, *Oscillators, Resonances and Lorentzians*, `http://www.toddsatogata.net/2013-USPAS/ResonantDrivenOscillator.pdf`, 2013.